PNAS RESEARCH ARTICLE | BIOCHEMISTRY OPEN ACCESS

HIV-1 prehairpin intermediate inhibitors show efficacy independent of neutralization tier

Benjamin N. Bell[a,b,1,2], Theodora U. J. Bruun[b,c,1], Natalia Friedland[b,c], and Peter S. Kim[b,c,d,3]

Contributed by Peter S. Kim; received September 19, 2022; accepted January 23, 2023; reviewed by Dennis R. Burton and Barton F. Haynes

HIV-1 strains are categorized into one of three neutralization tiers based on the relative ease by which they are neutralized by plasma from HIV-1–infected donors not on antiretroviral therapy; tier-1 strains are particularly sensitive to neutralization while tier-2 and tier-3 strains are increasingly difficult to neutralize. Most broadly neutralizing antibodies (bnAbs) previously described target the native prefusion conformation of HIV-1 Envelope (Env), but the relevance of the tiered categories for inhibitors targeting another Env conformation, the prehairpin intermediate, is not well understood. Here, we show that two inhibitors targeting distinct highly conserved regions of the prehairpin intermediate have strikingly consistent neutralization potencies (within ~100-fold for a given inhibitor) against strains in all three neutralization tiers of HIV-1; in contrast, best-in-class bnAbs targeting diverse Env epitopes vary by more than 10,000-fold in potency against these strains. Our results indicate that antisera-based HIV-1 neutralization tiers are not relevant for inhibitors targeting the prehairpin intermediate and highlight the potential for therapies and vaccine efforts targeting this conformation.

HIV-1 | tier-2 virus | tier-3 virus | 5-Helix | prehairpin intermediate

HIV-1 strains are routinely categorized into neutralization tiers based on the relative ease by which they are inhibited by HIV-1 antisera (1, 2), most likely by antibodies targeting Envelope (Env), the only viral protein on the surface of HIV-1 virions (3) (Fig. 1*A*). Tiered classification helps distinguish unusually sensitive strains in tier 1, such as those that are laboratory-adapted, from more difficult-to-neutralize strains in tiers 2 and 3 that are better representatives of currently circulating strains (1, 2) (Fig. 1*A*). This tiered system has also been used to systematically compare potential HIV-1 immunogens. A tier-1 neutralizing antibody response can be readily elicited by monomeric gp120 immunogens, but is not protective (4, 5); accordingly, eliciting a tier-2 neutralizing response has become the standard for evaluating prospective HIV-1 vaccine candidates (1, 2, 6–8). Recent efforts to precisely categorize strains by a continuous neutralization index (2) instead of in discrete tiers (i.e., Fig. 1 *A* and *B*, refs. 2 and 3) illustrate the utility of this tiered system to HIV-1 research and vaccine development.

The target of antibody-mediated neutralization, HIV-1 Env, undergoes a series of conformational changes upon receptor and coreceptor binding that enable viral membrane fusion through the formation of a trimer-of-hairpins conformation (13, 14, 22) (Fig. 1*B*). Most bnAbs that have been described previously target the native state of Env (23–25), though some bnAbs are reported to bind additional Env conformations (24). While such bnAbs have been challenging to elicit by HIV-1 vaccine candidates (6, 8, 26, 27), major efforts are underway to harness them for passive immunization campaigns including the recently reported Antibody Mediation Prevention trials (28–31), which showed that the bnAb VRC01 could prevent HIV-1 acquisition in healthy volunteers, but only for ~30% of viral strains encountered in the cohort (30). Although these trials and others show the feasibility of targeting prefusion Env in HIV-1 vaccine and therapeutic approaches, they nevertheless highlight the remaining challenges of HIV-1 prevention.

In addition to the native prefusion Env conformation, the prehairpin intermediate (PHI) of Env can also be targeted by HIV-1 therapeutics and vaccine candidates, including peptides (32–37), antibodies (19, 20, 38), and designed proteins (21) (Fig. 1*B*). Binding to the gp41 N- or C-heptad repeats (NHR and CHR, respectively) in the PHI prevents the formation of the trimer-of-hairpins (Fig. 1*B*) and is a validated inhibitory mechanism (13, 22), exemplified by the fusion inhibitor Fuzeon™/enfuvirtide, approved by the U.S. Food and Drug Administration (36, 37). Both the NHR and CHR are compelling targets, primarily due to their high sequence conservation among diverse viral clades; indeed, many positions in these regions have nearly 100% sequence identity among all known HIV-1 strains (13–15, 39). The NHR-targeting antibody D5_AR IgG was recently shown to weakly neutralize all strains in the tier-2 Global Reference Panel (at concentrations < 100 μg/mL) (20, 40) but with dramatic potentiation (>1,000-fold) in the presence of

Significance

HIV-1 strains are categorized into three tiers based on their sensitivity to neutralization by patient antisera, but it is poorly understood how these tiers influence the efficacy of inhibitors targeting the prehairpin intermediate (PHI) of HIV-1 glycoprotein Env. Here, we find that a PHI-targeting Ab and protein inhibitor have strikingly consistent neutralization potencies across all three tiers, whereas four broadly neutralizing antibodies (bnAbs) currently used in clinical trials show large variability against these viruses. Although PHI-targeting antibodies identified to date generally have modest neutralization potencies, our results demonstrate that the current system of classifying HIV-1 is not relevant for PHI-targeting HIV-1 vaccine efforts and strongly imply that such strategies can provide an especially broad layer of protection.

Author contributions: B.N.B., T.U.J.B., and P.S.K. designed research; B.N.B. and T.U.J.B. performed research; B.N.B., T.U.J.B., and N.F. contributed new reagents/analytic tools; B.N.B., T.U.J.B., and P.S.K. analyzed data; and B.N.B., T.U.J.B., and P.S.K. wrote the paper.

Reviewers: D.R.B., Scripps Research Institute; and B.F.H., Duke University.

The authors declare no competing interest.

[1]B.N.B. and T.U.J.B. contributed equally to this work.

[2]Present address: Merck & Co., Inc., South San Francisco, CA 94080.

[3]To whom correspondence may be addressed. Email: kimpeter@stanford.edu.

This article contains supporting information online at https://www.pnas.org/lookup/suppl/doi:10.1073/pnas.2215792120/-/DCSupplemental.

Published February 16, 2023.

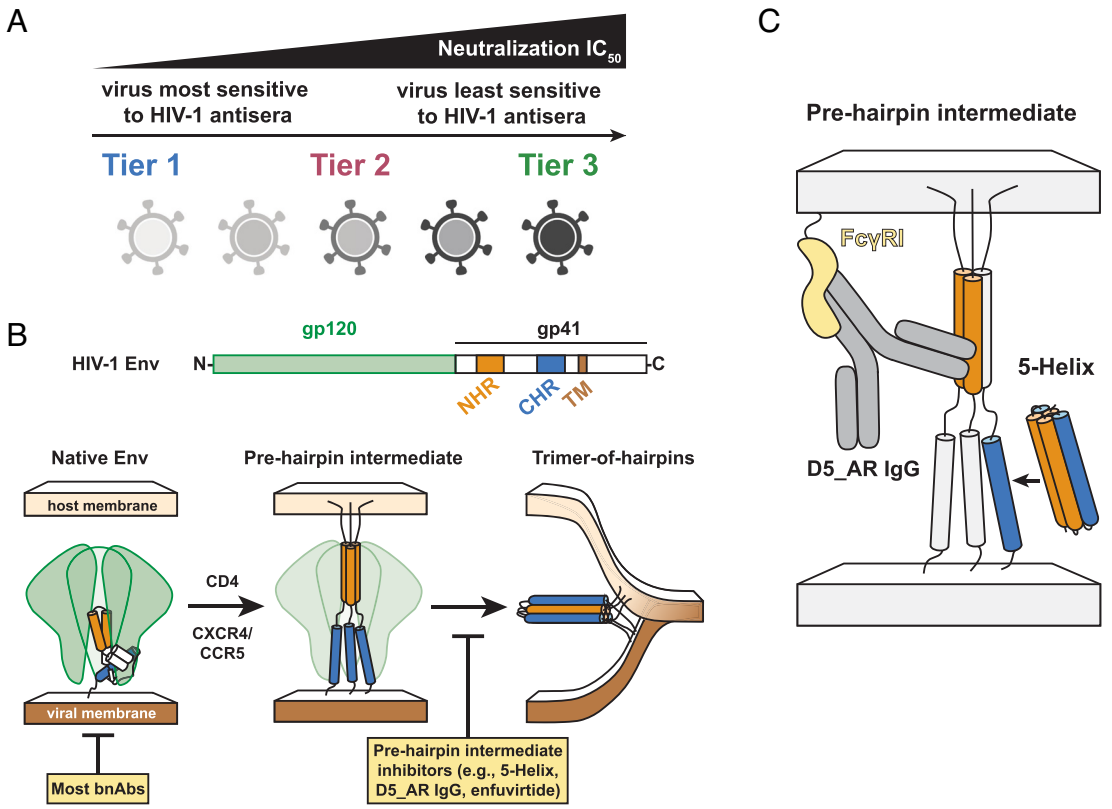

Fig. 1. The HIV-1 PHI represents an additional neutralization target. (*A*) HIV-1 strains are organized into neutralization tiers based on their sensitivity to patient sera: tier-1 strains are particularly sensitive to neutralization, while tier-2 and tier-3 strains are more resistant. (*B*) HIV-1 Env (linear schematic) is a transmembrane viral protein composed of a trimer of gp120/gp41 heterodimers. The native, prefusion conformation of Env (*Left*) engages cell-surface receptors CD4 and CCR5/CXCR4. The gp41 NHR and CHR are critical regions in membrane fusion exposed in the PHI (*Center*) before collapsing into a stable trimer-of-hairpins structure (*Right*). Env-directed inhibitors target either the native prefusion conformation (*Left*) or the PHI (*Center*). Most bnAbs target the native prefusion state, while fusion inhibitors like 5-Helix, D5_AR IgG, and enfuvirtide prevent the transition between the PHI and the trimer-of-hairpins structure. Cartoons are based on high-resolution crystal and cryogenic electron microscopy structures [Protein Data Bank codes: 5FUU (9), 6MEO (10), 1AIK (11), 2X7R (12) and a common model for the PHI (13–18). (*C*) The PHI inhibitors D5_AR IgG and 5-Helix target the NHR and CHR, respectively. D5_AR IgG binds a highly conserved hydrophobic pocket in the NHR trimeric coiled-coil (orange), and recent work has shown that the neutralization potency of D5_AR IgG is greatly enhanced >1,000-fold when target cells express Fc gamma receptor I (FcγRI; yellow) (19, 20). 5-Helix is an engineered protein designed to mimic the post-fusion trimer-of-hairpins structure and binds the highly conserved α-helical face of the CHR (blue) (21). Highly conserved residues are highlighted in red.

FcγRI receptors (19, 20) (Fig. 1*C*). The CHR-targeting designed protein called 5-Helix binds highly conserved CHR residues that form an α-helical conformation (39) (Fig. 1*C*); accordingly, 5-Helix has potent neutralizing activity at low nanomolar concentrations across distinct viral clades, though only a handful of viral strains have been examined to date (21, 41–44).

Despite the widespread use of the neutralization tier system to evaluate clinical approaches for HIV-1, it remains poorly understood whether such tiers predict resistance and sensitivity to inhibitors targeting the PHI (45). Here, we determined how the neutralization potencies of D5_AR IgG and 5-Helix compare among viral strains across neutralization tiers. We ranked a panel of 18 viral strains according to neutralization tier using pooled HIV-1 antisera (Anti-HIV immunoglobulin or HIVIG) and evaluated the potency of bnAbs targeting various Env epitopes that are being evaluated in passive immunization clinical trials: VRC01 (25, 30), PGDM1400 (31, 46), 3BNC117 (29, 47), 10-1074 (28, 48), and 10E8v4 (31, 49). We find that D5_AR IgG and 5-Helix have broad and consistent neutralization potencies across neutralization tiers and viral clades (within ~100-fold), in marked contrast to the best-in-class bnAbs targeting prefusion Env epitopes, which vary by over 10,000-fold in potency. These results suggest that HIV-1 neutralization tiers as they are currently defined are not relevant to inhibitors targeting the PHI and further highlight the appeal of HIV-1 therapeutics and vaccines that target the Env PHI.

Results

Inhibitors Targeting the PHI Have Broad Activity across Neutralization Tiers. HIV-1 neutralization tiers separate strains that are more sensitive to inhibition by sera (tier 1) from those that are more resistant to neutralization (tiers 2 and 3) but have not been evaluated in the context of inhibitors targeting the PHI. To readily compare neutralization activities across tiers and between different inhibitors and bnAbs, we first produced a panel of HIV-1 Env-pseudotyped lentiviruses representing strains that span clades and neutralization tiers including the tier-2 Global Reference Panel (40) and select tier-1 and tier-3 strains (Table 1). We also chose to employ the widely used TZM-bl cell line, which has become the standard for assessing HIV-1 serum neutralization (40, 50–53).

Although 5-Helix neutralization activity has been reported using a number of cell-cell fusion (21, 41) and virus-cell fusion (41–44) assays, no reports to date have employed TZM-bl cells. Therefore, we first sought to determine 5-Helix potencies using TZM-bl cells and corroborate our findings using HOS-CD4-CCR5 target cells for which 5-Helix potencies have been published (41–44). We validated our 5-Helix preparations biochemically (*SI Appendix*, Fig. S1 *A–G*) and found good agreement between our half-maximal inhibitory concentration (IC_{50}) value using HOS-CD4-CCR5 cells and HXB2 Env-pseudotyped

Table 1. Neutralization potencies of PHI inhibitors 5-Helix and D5_AR IgG against HIV-1 panel

			5-Helix, IC_{50} (μg/mL)		D5_AR IgG, IC_{50} (μg/mL)[29]		D5_AR IgG, IC_{50} (μg/mL); FcγRI-expressing cells	
Strain	Tier	Clade	Average	SD	Average	SD	Average	SD
MW965.2	1	C	0.88	0.38	2.5	0.04	0.004	0
SF162	1	B	2.7	0.21	40	15	0.01	0
HXB2	1	B	1.1	0.25	5.4	1.0	0.007	0
BaL	1	B	3.5	0.5	26	8.3	0.045	0.0071
SS1196.1	1	B	1.9	1.4	23	10	0.025	0.0071
25710	2	C	1.9	0.24	4.6	0.7	0.014	0
TRO.11	2	B	1.5	0.25	54	14	0.025	0.0071
BJOX2000	2	CRF07_BC	1.4	0.22	46	6.0	0.008	0.0014
X1632	2	G	3.0	0.72	66	8.0	0.035	0.0071
CE1176	2	C	2.8	0.71	79	10	0.15	0.071
246F3	2	AC	2.3	0.35	28	1.9	0.015	0.0071
CH119	2	CRF07_BC	2.2	0.29	37	4.7	0.06	0.028
CE0217	2	C	2.2	0.069	27	6.0	0.025	0.0071
CNE55	2	CRF01_AE	5.2	0.87	26	2.2	0.02	0.014
TRJO	3	B	1.6	0.38	29	14	0.065	0.0071
33-7	3	CRF02_AG	1.2	0.18	29	0.21	0.02	0
PVO.4	3	B	5.9	0.52	34	0.27	0.035	0.0071
253-11	3	CRF02_AG	0.51	0.099	12	1.0	0.0065	0.00071

lentivirus (8.2 ± 4.1 nM; *SI Appendix*, Fig. S2*A*), compared to a previously published value using this strain and cell line [11 ± 1.2 nM (41). We observed a reduction in 5-Helix neutralization potency using TZM-bl cells compared to HOS-CD4-CCR5 cells across multiple strains (*SI Appendix*, Fig. S2*A*), in line with similarly enhanced activity in HOS-CD4-CCR5 over TZM-bl target cells observed with NHR-targeting inhibitors HK20, D5, and Fuzeon™/enfuvirtide (38). Such discrepancies across neutralization assay formats are well documented (54), likely due to differences in viral membrane fusion in these cell lines.

We next evaluated 5-Helix neutralization potency against strains across HIV-1 neutralization tiers. Of note, 5-Helix had broad activity across neutralization tiers and viral clades in a narrow range of IC_{50} values (~10-fold), including potent inhibition of three of the four tier-3 strains tested (<80 nM or <2 μg/mL; Fig. 2*A* and Table 1). Indeed, one tier-3 strain, 253-11, characterized as being unusually resistant to neutralization (55), was especially sensitive to inhibition by 5-Helix (Fig. 2*A* and Table 1). To validate that the observed sensitivity to 5-Helix was not an artifact of our tier-3 pseudovirus preparations, we tested these strains against the bnAb 10E8v4 IgG1 and found close agreement with published values (56) (*SI Appendix*, Fig. S2*B*), indicating that this sensitivity to 5-Helix is genuine.

As the PHI can be inhibited by targeting either the CHR or the NHR, we next used our pseudovirus panel to evaluate the neutralization potencies of the NHR-targeting antibody D5_AR IgG, which was first described to weakly neutralize all strains in the tier-2 Global Reference Panel (20, 40). We found similar potencies for D5_AR IgG and also saw at least 1,000-fold increases in neutralization potency in the presence of the cell-surface receptor FcγRI as previously described (19, 20) (Fig. 2*B*). Like 5-Helix, D5_AR IgG also showed a narrow range of IC_{50} values (~100-fold) that did not correlate well with neutralization tier (Fig. 2*B*).

As the neutralization tier does not seem to account for variable sensitivity to 5-Helix and D5_AR IgG, we considered whether differing binding affinities of 5-Helix to CHR sequences correspond to differing sensitivities among strains. The NHR mutation L565Q does not affect the CHR sequence; thus, one might expect 5-Helix would show similar neutralization potency in the presence or absence of the mutation. However, the L565Q virus showed increased sensitivity to 5-Helix (Fig. 2*C*), in line with previous reports (44, 57), indicating that epitope sequence is not the only determinant of sensitivity to 5-Helix. To further probe how sequence diversity impacts 5-Helix efficacy, we next assayed 5-Helix binding to nine peptides representing the CHR sequences of some of the strains tested across viral clades in our panel (Fig. 2*D* and *SI Appendix*, Table S1). Due to the extremely high affinity of 5-Helix for the CHR [K_D = 0.6 pM in the case of HXB2 (41)], we measured binding affinity by biolayer interferometry using steady-state values after 1 h of association in the presence of 1 M guanidine hydrochloride (*SI Appendix*, Fig. S3 *A–I*). Consistent with our observations of HXB2 vs. HXB2 L565Q (Fig. 2*C*), there was not a strong correlation between 5-Helix binding affinity for various CHR sequences and IC_{50} values (Fig. 2*D*).

As the CHR sequence alone does not fully determine strain sensitivity to 5-Helix, we next considered whether there is a correlation between strains that were sensitive to 5-Helix and those sensitive to D5_AR IgG. Previous studies using 5-Helix and CHR-peptide mutants proposed that the CHR and NHR have distinct windows of vulnerability and accessibility in the PHI (41). Indeed, we found poor agreement between strains that were sensitive to inhibition by 5-Helix and those sensitive to inhibition by D5_AR IgG, with poor linear correlation (R^2 = 0.06; Fig. 2*E*). Additionally, D5_AR IgG IC_{50} values span a slightly larger range than those of 5-Helix (100-fold vs. 10-fold; Fig. 2*E* and Table 1). Therefore, strain sensitivity to PHI inhibitors is not explained by differences in target binding affinity (Fig. 2 *C* and *D*), nor do the NHR and CHR have equal susceptibility (Fig. 2*E*).

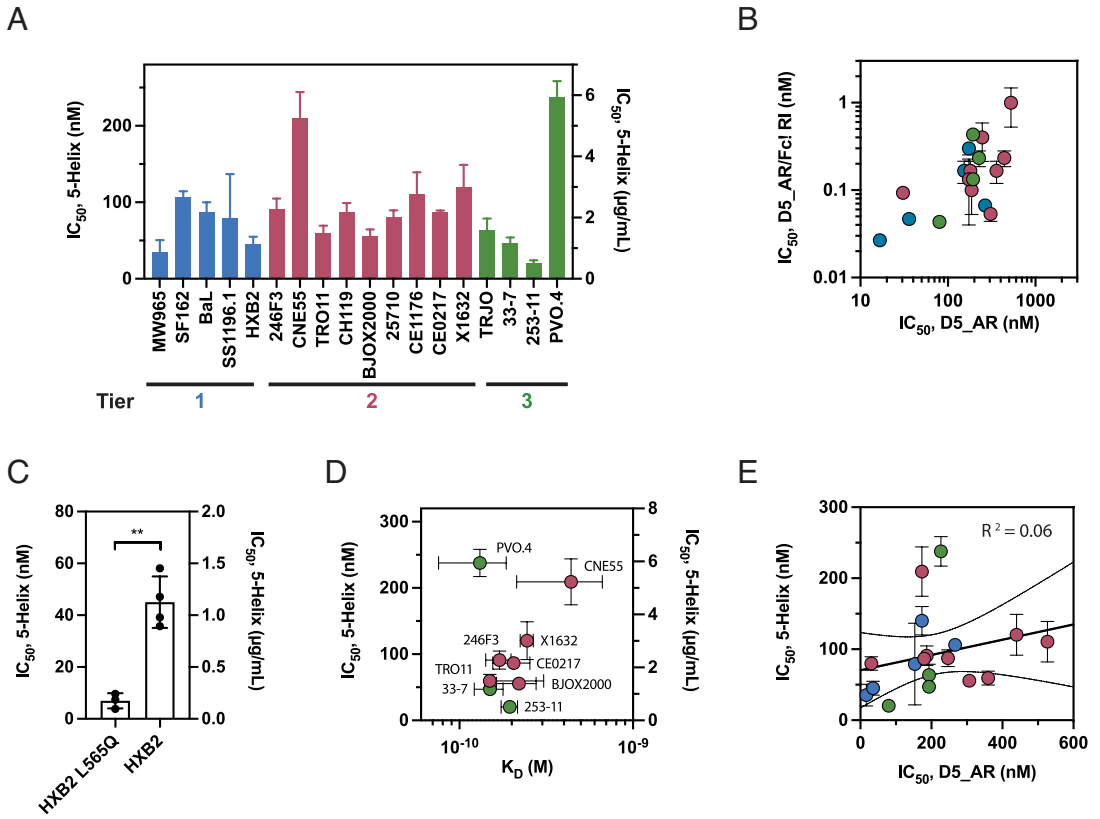

Fig. 2. Inhibitors targeting the PHI have broad activity across neutralization tiers. (*A*) CHR-targeting inhibitor 5-Helix shows activity across a roughly 10-fold range against viral strains in neutralization tiers 1/2/3. In *A–E*, IC_{50} values from TZM-bl neutralization assays performed in biological triplicate are plotted as mean ± SD and colored by neutralization tier: tier 1 (blue), tier 2 (red), and tier 3 (green). (*B*) NHR-targeting D5_AR IgG shows activity against viral strains in neutralization tiers 1/2/3 that is potentiated roughly 1,000-fold for cells expressing FcγRI. Mean IC_{50} values ± SD of repeated neutralization assays done in at least biological triplicate using either TZM-bl (*x*-axis) or TZM-bl/FcγRI (*y*-axis) cells are shown. (*C*) HIV-1 strains with identical CHR sequences (HXB2 and HXB2 L565Q) show differences in 5-Helix sensitivity. Two-tailed unpaired *t* tests were performed with the indicated *P* value (**$P < 0.01$). (*D*) Increased binding of 5-Helix to CHR sequences measured by biolayer interferometry does not correspond to increased sensitivity to inhibition by 5-Helix. Reported K_D values (mean ± SD) were determined from repeated experiments (n = 2) for each peptide across a range of concentrations of 5-Helix. (*E*) Sensitivity to 5-Helix does not predict sensitivity to D5_AR IgG. IC_{50} values of 5-Helix and D5_AR IgG fall over notably different ranges and show only a modest association. A linear regression (black) with 95% confidence bands (dashed) has a correlation coefficient of $R^2 = 0.06$.

PHI Inhibitors Show Highly Consistent and Broad HIV-1 Neutralization Independent of Tier, Unlike Best-in-Class bnAbs

We sought to determine whether the broad, narrow range of potencies we observed for 5-Helix and D5_AR IgG were unique; accordingly, we assayed our 18-virus panel in neutralization assays using best-in-class bnAbs currently employed in clinical trials: 10E8v4 [targeting the gp41 membrane-proximal external region (MPER) (31, 49)], VRC01 (30) and 3BNC117 (29) (targeting the CD4 binding site in gp120), PGDM1400 (31) (targeting the gp120 V1/V2 apex), and 10-1074 (28) (targeting the gp120 V3 loop). We used HIVIG (purified immunoglobin from pooled HIV-1 patient sera) as a quantitative representation of neutralization tier, as similar pools of patient sera are used to delineate these tiers (Table 2) (2, 45).

We found striking differences between the gp120 bnAbs evaluated here and 5-Helix or D5_AR IgG (Fig. 3*A*). The neutralization potencies of 5-Helix and D5_AR IgG did not vary substantially across a wide range of HIVIG potencies (13 to >2,500 μg/mL), whereas the four bnAbs varied widely (Fig. 3*A*). We quantified the variation in IC_{50} values by examining the log-values of the interquartile range (IQR) as well as the total range of the data (Fig. 3*B*). While 5-Helix and D5_AR IgG IC_{50} values varied by up to two logs (~100-fold), the clinical gp120-targeting bnAbs tested showed ranges of ~10,000-fold (VRC01) to nearly 100,000-fold (3BNC117, 10-1074; Fig. 3 *A* and *B*). Notably, the gp41-targeting bnAb 10E8v4 showed similarly narrow neutralization potencies as D5_AR and 5-Helix among tier-2/3 strains. The MPER is also preferentially exposed in the PHI conformation of gp41 (59, 60), further corroborating the unique differences between gp41- and gp120-targeting inhibitors. Taken together, these results show that neutralization tiers have minimal predictive power for inhibition by 5-Helix and D5_AR IgG; further, such inhibitors show extremely narrow ranges of IC_{50} values unlike best-in-class bnAbs currently employed in clinical studies.

Discussion

HIV-1 neutralization tiers are a powerful tool to evaluate novel strains and vaccine candidates (40, 45) as the neutralization activity of bnAbs and vaccine sera can vary substantially against tier-2 and tier-3 strains. Here, we show that 5-Helix and D5_AR IgG, two inhibitors targeting highly conserved gp41 epitopes in the PHI, can have broad inhibitory activity against strains in all three neutralization tiers of HIV-1, including particularly resistant tier-3 strains (Fig. 2*A* and Table 1). Although 5-Helix and D5_AR IgG neutralization potencies are modest (10 to 1,000 nM, Fig. 3*A*), they show very narrow variation across tiers (less than ~100-fold), unlike best-in-class bnAbs currently employed in clinical trials (more than 10,000-fold, Fig. 3 *A* and *B*) (28–31). Notably, even though D5_AR is a generally weak inhibitor

Table 2. Neutralization potencies of best-in-class bnAbs against HIV-1 panel

			HIVIG, IC_{50} (μg/mL)			VRC01, IC_{50} (μg/mL)			3BNC117, IC_{50} (μg/mL)		
Strain	Tier	Clade	Average	SD	Reported*	Average	SD	Reported*	Average	SD	Reported*
MW965.2	1	C	26	13	<0.02	0.075	0.0071	0.03	0.035	0.01	0.006
SF162	1	B	13	5	6	0.3	0.028	0.15	0.04	0	0.02
HXB2	1	B	59	13	28	0.12	0.014	0.03	0.11	0.04	0.03
BaL	1	B	150	56	69	0.13	0.049	0.08	0.01	0	0.01
SS1196.1	1	B	400	90	191	0.47	0.18	0.24	0.055	0.021	0.03
25710	2	C	700	14	NR†	1	0.14	0.53	0.33	0.11	0.13
TRO.11	2	B	470	180	705	0.42	0.0071	0.33	0.03	0	0.04
BJOX2000	2	CRF07_BC	1,600	220	NR†	83	7.9	>50	>150	–	>50
X1632	2	G	2,300	39	NR†	0.26	0.042	0.11	3.9	3.3	4
CE1176	2	C	2,400	150	NR†	4.9	0.29	2.1	0.49	0.12	0.22
246F3	2	AC	1,600	69	NR†	0.69	0.0071	0.27	0.32	0.11	NR†
CH119	2	CRF07_BC	1,400	270	2,236	2.3	0.071	0.71	7.9	1.1	4.8
CE0217	2	C	>2,500	–	NR†	0.53	0.099	0.23	0.08	0.028	0.04
CNE55	2	CRF01_AE	>2,500	–	NR†	0.5	0.11	0.34	0.13	0.064	0.12
TRJO	3	B	1,010	83	1,221	0.12	0.014	0.088	0.15	0	0.066
33-7	3	CRF02_AG	1,020	150	1,900	0.01	0	0.02	0.004	0.0028	0.006
PVO.4	3	B	890	280	1,277	0.73	0.11	0.45	0.065	0.0070	0.06
253-11	3	CRF02_AG	1,550	350	>2,500	0.56	0.0071	0.39	0.16	0.042	0.1

	PGDM1400, IC_{50} (μg/mL			10-1074, IC_{50} (μg/mL)			10E8v4, IC_{50} (μg/mL)			VRC01, IC_{80}‡ (μg/mL)
Strain	Average	SD	Reported*	Average	SD	Reported*	Average	SD	Reported*	Reported*
MW965.2	0.015	0.0071	0.03	0.02	0	0.005	0.03	0	0.003	0.11
SF162	0.71	0.21	0.29	0.006	0.0014	0.001	1.9	0.35	0.55	0.65
HXB2	34	6.2	>50	34	5.7	3.9	0.009	0.0014	0.003	0.1
BaL	1.8	0.071	0.09	0.06	0	0.006	2.3	0.14	0.3	0.28
SS1196.1	0.75	0.071	0.19	0.01	0	0.002	0.6	0	0.13	0.69
25710	0.0035	0.00071	0.006	0.07	0.028	0.02	0.09	0.014	0.04	1.6
TRO.11	0.46	0.19	0.5	0.11	0.057	0.01	0.55	0.071	0.11	1.2
BJOX2000	0.03	0.014	0.002	0.01	0	0.01	0.63	0.11	0.45	>50
X1632	0.025	0.0071	0.007	>150	–	>50	1.7	0.14	0.31	0.66
CE1176	0.57	0.18	0.11	0.055	0.021	0.02	0.5	0	0.4	6.1
246F3	0.008	0.0014	0.003	>150	–	NR†	0.8	0	0.27	0.7
CH119	0.35	0.071	0.06	0.035	0.0071	0.016	0.45	0.071	0.7	2.5
CE0217	0.008	0.0014	0.003	0.015	0.0071	0.005	0.12	0.028	0.15	0.75
CNE55	0.0085	0.0021	0.01	>150	–	>50	0.8	0	0.09	1.1
TRJO	50.0	1.7	>100	0.85	0.071	0.13	3.2	0.85	2.4	0.26
33-7	0.0095	0.00071	0.001	>150	–	>50	1.0	0.071	0.86	0.04
PVO .4	1.3	0.21	1.2	0.375	0.0071	0.06	4.7	0.35	2.6	1.3
253-11	0.015	0.0071	0.006	3	0.71	2.7	0.55	0.21	0.8	1.0

*Values published in the HIV-1 CATNAP database (66) (www.hiv.lanl.gov).
†Not reported.
‡80% inhibitory concentration

of HIV-1 infection, dramatic potentiation observed in the presence of FcγRI suggests that more robust neutralization activity might occur in vivo (20, 61); although target CD4+ T cells lack FcγRI expression, macrophages and dendritic cells at mucosal surfaces are infected in the earliest stages of sexual HIV-1 transmission (62–67) and do bear cell-surface FcγRI expression (19). Further, despite its relatively weak inhibition overall, D5_AR IgG still showed superior neutralization potency compared to the bnAbs studied here to some tier-2 (BJOX2000, X1632, 246F3, CNE55) and tier-3 (TRJO, 33-7) strains (Fig. 3*A*, Table 1, and *SI Appendix*, Table S1). Overall, these results indicate that inhibitors targeting the PHI show efficacy independent of HIV-1 neutralization tiers.

The current model for the molecular basis of HIV-1 neutralization tiers posits that sensitivity to patient antiserum corresponds to the likelihood of prefusion Env occupying the "open" conformation on the surface of virions; Env trimers that frequently sample the open conformation tend to be easier to neutralize (tier 1), while those that are more stably "closed" are more difficult to neutralize (tier 3) (45, 55). There has been some experimental evidence of this using single-molecule Förster resonance energy transfer (FRET) of Env on intact

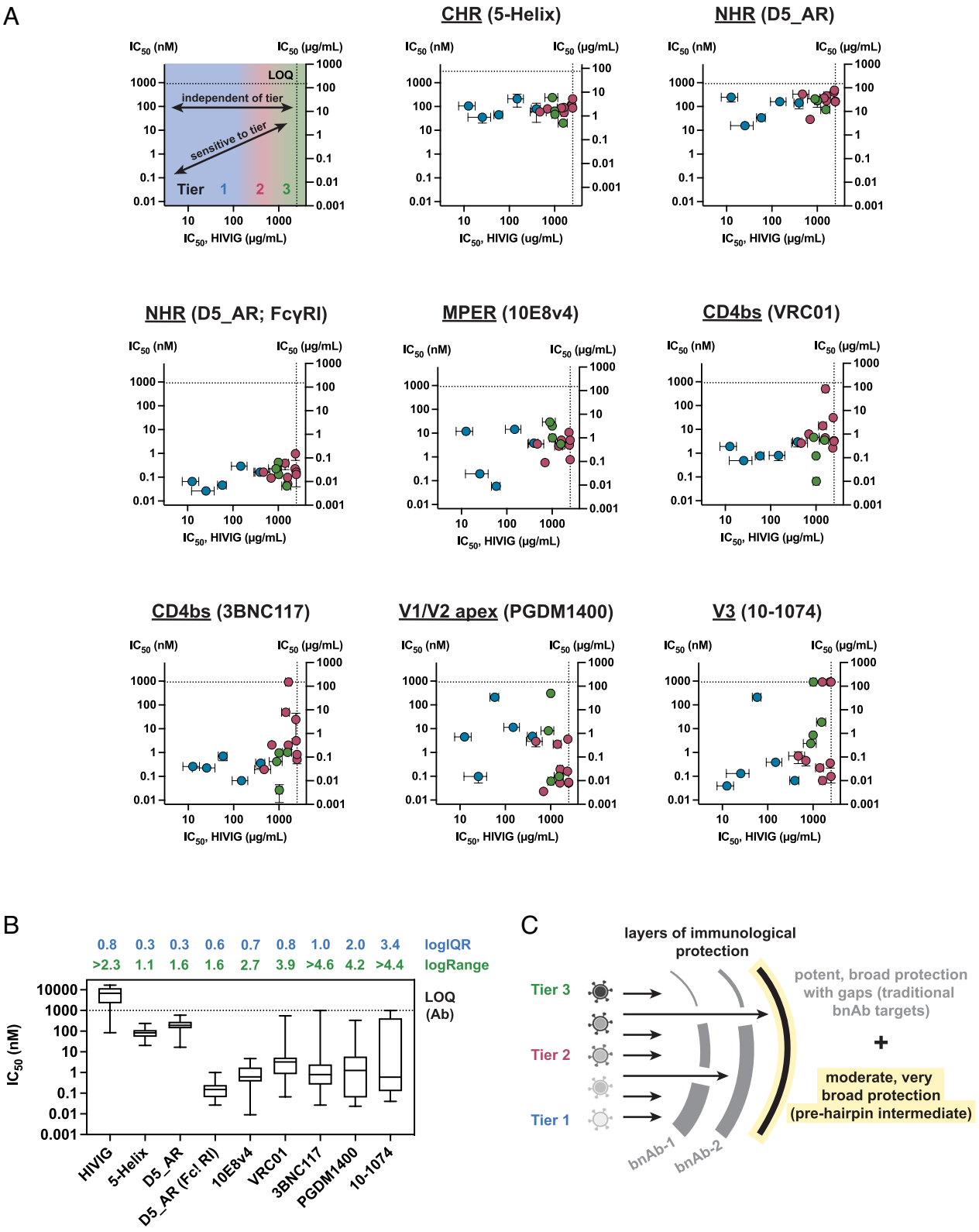

Fig. 3. PHI inhibitors show highly consistent and broad HIV-1 neutralization independent of tier, unlike best-in-class bnAbs. (*A*) 5-Helix and D5_AR IgG show highly consistent neutralization activity across tiers. Neutralization IC_{50} values were determined against a panel of tier-1/2/3 strains for immunoglobin purified from pooled HIV-1 sera (HIVIG) and five bnAbs employed in clinical trials 10E8v4, VRC01, 3BNC117, PGDM1400, and 10-1074. Using HIVIG as an indicator of tier, only 5-Helix and D5_AR IgG (in TZM-bl cells ± FcγRI expression) show highly consistent activity among strains across tiers. The limit-of-quantitation (LOQ) is indicated by dashed lines. Values are plotted as mean ± SD and colored by neutralization tier: tier 1 (blue), tier 2 (red), and tier 3 (green). Epitopes of each inhibitor are indicated: MPER, CD4 binding site (CD4bs), gp120 V1/V2 apex, and gp120 V3 loop. (*B*) Box-and-whisker plots of IC_{50} values in *A* show that 5-Helix and D5_AR IgG have narrower ranges than HIVIG or best-in-class bnAbs. The logarithms of the IQR and the range are reported. The LOQ for the antibody neutralization datasets is indicated by the dashed line. (*C*) Proposed model for incorporating inhibitors targeting the PHI into current HIV-1 prevention approaches. Viruses from different neutralization tiers show different susceptibility to current best-in-class bnAbs but similar vulnerability to inhibitors targeting the PHI. High neutralization potency is represented as thicker layers of protection with no potency represented as a gap in the layer. Eliciting antibodies that neutralize via the PHI may provide an additional layer of protection that would be useful even if moderate but very broad.

virions wherein Env occupies distinct FRET states that correspond to neutralization tier (68, 69). Further, this model is compatible with bnAbs targeting gp120, which itself undergoes these conformational changes in the prefusion state (69).

It is noteworthy that gp41-targeting inhibitors (i.e., 10E8v4, D5_AR, and 5-Helix) showed more similarity in neutralization potencies across tier-2/3 strains than the gp120-targeting bnAbs tested (Fig. 3*A*). It is possible that prefusion conformational dynamics that correspond well to HIV-1 neutralization tiers have little bearing on the ability of gp41-targeting inhibitors to bind their targets since these epitopes are only exposed later during membrane fusion. Other factors that may impact the differences between gp120-targeting and gp41-targeting inhibitors we observe here include higher sequence conservation in PHI epitopes compared to gp120 (20, 21, 39), as well as dense and varied glycosylation in gp120 that is not as present in gp41 (7, 27, 48).

If neutralization tiers do not predict sensitivity to PHI inhibitors, what factors may be at play? Differences in the binding affinities between 5-Helix and distinct CHR sequences did not account for differences in sensitivity to inhibition by 5-Helix (Fig. 2 *C* and *D*). Targeting the NHR and CHR does not appear to be equivalent: we observed a wider range of IC_{50} values for D5_AR IgG compared to 5-Helix, and strains more resistant to 5-Helix were not necessarily more resistant to D5_AR IgG (Fig. 2*E*). The PHI is a transient structure, and its lifetime may vary among strains; it is therefore possible that different fusion kinetics could affect inhibitor access and efficacy. Indeed, mutations in the gp41 NHR that showed resistance to Fuzeon™/enfuvirtide conferred delayed viral membrane fusion kinetics (57, 70), and such mutations sensitize strains to inhibition by 5-Helix (44) (e.g., HXB2 L565Q, Fig. 2*C*). Further, differences in steric (71, 72) and kinetic (41–43) accessibility of the NHR and CHR peptide variants. These hypotheses warrant future study to identify the determinants of differing sensitivity to PHI inhibitors.

Current bnAbs used in the clinic have shown the promise of passive immunization approaches (28–31), but the large fraction of resistant viruses encountered already in these trials highlights the challenge of gaps in which these bnAbs do not provide protection (Fig. 3*C*). Indeed, in recent trials using VRC01, nearly 70% of participants were infected by strains with at least some resistance to VRC01 neutralization (defined as $IC_{80} \geq 1$ μg/mL) (30). Pharmacokinetic estimates suggest that participants had average VRC01 serum concentrations of 10 to 30 μg/mL throughout the study period (see Supplemental Appendix of ref. 19); recent modeling estimates that 90% protection from infection corresponded to VRC01 serum titers at least 200-fold greater than in vitro neutralization IC_{80} values (73). Based on these considerations, a large majority of the tier-2/3 strains in our panel would be predicted to infect VRC01-trial participants (30, 58) (Table 2; last column). While current inhibitors against the PHI would not fare better than clinical bnAbs at these concentrations, the narrow range of IC_{50} values we observe suggest these targets have the potential to provide a very broad layer of protection not afforded by current bnAbs (Fig. 3*C*).

Developing a vaccine that protects against clinical HIV-1 isolates (i.e., tier-2 and tier-3 strains) remains a significant challenge. Our results demonstrate that inhibitors targeting the PHI conformation of HIV-1 Env are strikingly less influenced by neutralization tier compared to best-in-class bnAbs. This suggests that vaccine strategies that successfully elicit antibodies targeting the PHI could provide an especially broad layer of protection. Further, this protection could be even more effective if FcγRI enhancement observed for gp41-targeting Abs and serum (19, 74–76) proves to be relevant in vivo, especially in macrophages and dendritic cells bearing this receptor. Overall, this work highlights the appeal of creating an HIV-1 vaccine that can elicit anti-CHR and/or anti-NHR neutralizing antibodies mimicking the broad binding and neutralization properties of 5-Helix and D5_AR IgG.

Materials and Methods

NIH HIV Reagents. The following reagents were obtained through the NIH HIV Reagent Program, Division of AIDS, National Institute of Allergy and Infectious Diseases (NIAID), and NIH: 1) Polyclonal Anti-HIV Immune Globulin, Pooled Inactivated Human Sera, ARP-3957, contributed by National Agri-Food Biotechnology Institute and National Heart Lung and Blood Institute (Dr. Luiz Barbosa); 2) HOS CD4+ CCR5+ Cells, ARP-3318, contributed by Dr. Nathaniel Landau, Aaron Diamond AIDS Research Center, The Rockefeller University; 3) TZM-bl Cells, ARP-8129, contributed by Dr. John C. Kappes, Dr. Xiaoyun Wu, and Tranzyme Inc.; 4) Panel of Global HIV 1 Env Clones, ARP-12670, from Dr. David Montefiori; 5) Vector pSV7d Expressing HIV-1 HXB2 Env (pHXB2-env), ARP-1069, contributed by Dr. Kathleen Page and Dr. Dan Littman; 6) HIV-1 93MW965.26 gp160 Expression Vector (pSVIII-93MW965.26), ARP-3094, contributed by Dr. Beatrice Hahn; 7) HIV-1 BaL.26 Env Expression Vector, ARP-11446, contributed by Dr. John Mascola; 8) HIV-1 SF162 gp160 Expression Vector, ARP-10463, contributed by Dr. Leonidas Stamatatos and Dr. Cecilia Cheng-Mayer; 9) Plasmid pcDNA3.1 D/V5-His TOPO© Expressing HIV-1 Env/Rev, ARP-11020, contributed by Dr. David Montefiori and Dr. Feng Gao; 10) HIV-1 Panel of HIV-1 Subtype A/G Env Clones, ARP-11673, contributed by Drs. D. Ellenberger, B. Li, M. Callahan, and S. Butera; 11) Panel of HIV-1 Subtype B Env Clones, ARP-11227, contributed by Drs. D. Montefiori, F. Gao, M. Li, B.H. Hahn, X. Wei, G.M. Shaw, J.F. Salazar-Gonzalez, D.L. Kothe, J.C. Kappes, and X. Wu. 12) The following reagent was obtained through the NIH HIV Reagent Program, Division of AIDS, NIAID, NIH: HIV-1 SG3ΔEnv Non-infectious Molecular Clone, ARP-11051, contributed by Dr. John C. Kappes and Dr. Xiaoyun Wu; 13) Vector CMV/R Containing the Human IgG1 Heavy Chain Gene for Expression of Anti-HIV-1 gp41 Monoclonal Antibody 10E8v4 in 293-6E Cells, ARP-12866, contributed by Dr. Peter Kwong; 14) Vector CMV/R Containing the Human IgG1 Light Chain Gene for Expression of Anti-HIV-1 gp41 Monoclonal Antibody 10E8v4 in 293-6E Cells, ARP-12867, contributed by Dr. Peter Kwong; 15) Anti-HIV-1 gp120 Monoclonal Antibody (3BNC117), ARP-12474, contributed by Dr. Michel Nussenzweig; 16) Anti-HIV-1 gp120 Monoclonal antibody (10-1074), ARP-12477, contributed by Dr. Michel Nussenzweig; 17) HIV-1 VRC01 Monoclonal Antibody Heavy Chain Expression Vector, ARP-12035, contributed by John Mascola; and 18) HIV-1 VRC01 Monoclonal Antibody Light Chain Expression Vector, ARP-12036, contributed by John Mascola.

5-Helix Expression/Purification. 5-Helix was recombinantly expressed and purified as previously described (21). Briefly, a 6-Helix construct was expressed recombinantly in BL21 (DE3) *Escherichia coli* (New England Biolabs). This construct was composed of three NHR and three CHR peptides with intervening glycine/serine linkers and a C-terminal hexahistidine purification tag. The final glycine/serine linker contained an arginine residue sensitive to trypsin cleavage. *E. coli* cultures were induced at OD_{600} ~0.6 to 0.8 with 1 mM isopropyl β-D-1-thiogalactopyranoside and harvested after 3 h expression at 37 °C shaking at 225 rpm.

Cell pellets were lysed via sonication in Tris-buffered saline [TBS: 25 mM Tris-HCl (pH 8.0), 100 mM NaCl] and bound to 1 mL Ni-NTA agarose (Ni^{2+}-coupled nitrilotriacetic acid agarose; Thermo Fisher Scientific) for 2 h at 4 °C with agitation. Subsequently, 6-Helix was eluted from the Ni-NTA resin with TBS + 250 mM imidazole (pH 8.0) following a wash with TBS + 25 mM imidazole (pH 8.0). Eluted protein was digested with trypsin (1:200 w/w) for 15 to 20 min in a shaking-platform incubator at 37 °C shaking at 100 rpm.

Trypsin-digested 6-Helix protein was then purified by high-pressure liquid chromatography (HPLC) on a C18 semipreparative column (Phenomenex) over a 38 to 45% acetonitrile gradient in the presence of 0.1% trifluoroacetic acid, and 5-Helix-containing HPLC fractions were analyzed by SDS-PAGE (sodium dodecyl-sulfate polyacrylamide gel electrophoresis) and pooled. Pooled fractions were diluted with TBS and 8 M urea (pH 8.0) to a final protein concentration of ~0.1 to 0.2 mg/mL and residual 6-Helix and CHR peptide were removed by binding to Ni-NTA resin for 1 h. The flow-through from this step was dialyzed overnight into phosphate buffered saline (PBS;pH 7.4). Following two additional 2 h dialysis steps into PBS, 5-Helix was concentrated to 2 mg/mL and flash frozen with liquid

nitrogen with 10% glycerol. A final gel-filtration chromatography purification step was performed using a Superdex 200 Increase 10/300 GL column (Cytiva) on a Cytiva ÄKTA Pure system immediately before use.

The 6-Helix protein sequence used to generate 5-Helix protein is MQLLSGIVQQQNNLLRAIEAQQHLLQLTVWGIKQLQARILAGGSGGHTTWMEWDREINNYTSLIHSLIEESQNQQEKNEQELLEGSSGGQLLSGIVQQQNNLLRAIEAQQHLLQLTVWGIKQLQARILAGGSGGHTTWMEWDREINNYTSLIHSLIEESQNQQEKNEQELLEGSSGGQLLSGIVQQQNNLLRAIEAQQHLLQLTVWGIKQLQARILAGGRGGGHTTWMEWDREINNYTSLIHSLIEESQNQQEKNEQELLEGGHHHHHH. The 5-Helix protein sequence is MQLLSGIVQQQNNLLRAIEAQQHLLQLTVWGIKQLQARILAGGSGGHTTWMEWDREINNYTSLIHSLIEESQNQQEKNEQELLEGSSGGQLLSGIVQQQNNLLRAIEAQQHLLQLTVWGIKQLQARILAGGSGGHTTWMEWDREINNYTSLIHSLIEESQNQQEKNEQELLEGSSGGQLLSGIVQQQNNLLRAIEAQQHLLQLTVWGIKQLQARILAGGR.

Antibody Expression/Purification. D5_AR, 10E8v4, VRC01, PGDM1400, and 10-1074 IgG1s were expressed and purified from Expi293F cells. Expression vectors for D5_AR were generated previously (20), expression vectors for VRC01 and 10E8v4 were sourced from the NIH HIV Reagent Program (see "NIH HIV Reagents"), and expression vectors for 10-1074 were gifted from Dr. Christopher Barnes (28, 48). PGDM1400 heavy and light chain sequences were synthesized (Integrated DNA Technologies) and cloned into a mammalian expression vector under a CMV promoter using InFusion (Takara) and sequence verified.

Expi293F cells were cultured in 33% Expi293 Expression/66% FreeStyle Expression medium (Thermo Fisher Scientific) and grown in baffled polycarbonate shaking flasks (Triforest) at 37 °C and 8% CO_2. Cells were grown to a density of ~3 × 10^6/mL and transiently transfected using FectoPro transfection reagent (Polyplus). For transfections, 0.5 μg total DNA (1:1 heavy chain to light chain plasmids) was added per mL final transfection volume to culture medium (1/10 volume of final transfection) followed by FectoPro at a concentration of 1.3 μL per mL final transfection volume and incubated at room temperature for 10 min. Transfection mixtures were added to cells, which were then supplemented with D-glucose (4 g/L final concentration) and 2-propylpentanoic (valproic) acid (3 mM final concentration). Cells were harvested 3 to 5 d after transfection via centrifugation at 18,000 × *g* for 15 min. Cell culture supernatants were filtered using a 0.22-μm filter prior to purification.

Filtered Expi cell culture supernatants were buffered with 1/10 volume 10× PBS and loaded onto a HiTrap MabSelect SuRe column (Cytiva) equilibrated in PBS (pH 7.4) using a Cytiva ÄKTA Pure system at a flow rate of 3.5 mL/min. The column was subsequently equilibrated with five column volumes PBS (pH 7.4) before elution with three column volumes 100 mM glycine (pH 2.8) into 1/10th volume of 1M Tris (pH 8.0). The column was washed with 0.5 M NaOH with a minimum contact time of 15 min between purifications of different antibodies. Elutions were concentrated using Amicon spin filters (molecular weight cut-off 10 kDa; Millipore Sigma) and were subsequently loaded onto a GE Superdex S200 increase 10/300 GL column preequilibrated in 1× PBS using a Cytiva ÄKTA Pure system. Protein-containing fractions were identified by A280 signal and/or SDS-PAGE, pooled, and stored at 4 °C or at −20 °C in 10% glycerol/1× PBS until use.

Env-Pseudotyped Lentivirus Production. Pseudotyped lentivirus bearing various HIV-1 Env proteins were produced by transient transfection of HEK293T cells (human embryonic kidney cell line). For standard TZM-bl assays, the pSG3ΔEnv backbone was used as described previously (20); for HOS-CD4-CCR5 assays, the pHAGE backbone was used instead as described elsewhere (77). Virus-containing media were harvested after 2 d, centrifuged, and 0.45-μm filtered. Virus infectivity was titered to ensure that similar levels of infection occurred across viruses and infectivity assays.

HOS-CD4-CCR5 Neutralization Assay. HOS-CD4-CCR5 cells (human osteosarcoma cell line stably expressing human CD4, CCR5, and low levels of CXCR4) were plated at a density of 5 × 10^3 cells per well in white-walled 96-well tissue culture plates (Greiner Bio-One 655098) in a growth medium [Dulbecco's Modified Eagle Medium, 10% fetal bovine serum (Gemini Bio-Products), 2 mM L-glutamine, 1% penicillin-streptomycin (Sigma-Aldrich), and 10 mM HEPES (4-(2-hydroxyethyl)-1-piperazineethanesulfonic acid; pH 7.0), 0.22-μm filter-sterilized]. The next day, media were removed and replaced with a 100-μL mixture of inhibitor in PBS, HIV-1 pseudotyped lentivirus in growth medium, and growth medium at a final concentration of 2.5 μg/mL diethylaminoethyl (DEAE)-dextran (Millipore Sigma). After 2 d, 50 μL was aspirated from the plates and 50 μL of BriteLite Luciferase Substrate (Perkin Elmer LLC) was mixed with each well. After 1 min incubation, luminescence was assayed on a Synergy BioHTX plate reader (BioTek). Neutralization IC_{50} values were determined using a three-parameter dose-response curve fit in Prism 9 software (GraphPad).

TZM-bl Neutralization Assay. TZM-bl neutralization assays were performed as described previously (20). Briefly, 5 × 10^3 TZM-bl cells (HeLa luciferase/β-galactosidase reporter cell line stably expressing human CD4, CCR5, and CXCR4) were plated per well in white-walled 96-well tissue culture plates (Greiner Bio-One 655098) in growth medium [Dulbecco's Modified Eagle Medium, 10% fetal bovine serum (Gemini Bio-Products), 2 mM L-glutamine, 1% penicillin-streptomycin (Sigma-Aldrich), 10 mM HEPES (pH 7.0), 0.22-μm filter-sterilized]. The next day, media were removed and replaced with a 100-μL mixture of inhibitor in PBS, HIV-1 pseudotyped lentivirus in growth medium, and growth medium at a final concentration of 10 μg/mL DEAE-dextran (Millipore Sigma). After 2 d, 50 μL was aspirated from the plates and 50 μL of BriteLite Luciferase Substrate (Perkin Elmer LLC) was mixed with each well. After 1 min incubation, luminescence was assayed on a Synergy BioHTX plate reader (BioTek). Neutralization IC_{50} values were determined using a three-parameter dose-response curve fit in Prism 9 software (GraphPad).

Peptide Synthesis. CHR peptides used for biolayer interferometry were synthesized by standard Fmoc-based solid-phase peptide synthesis (China Peptides Co. Ltd.). Peptides were modified to contain an N-terminal biotin-PEG6 (polyethylene glycol) linker and a C-terminal amide group. Peptides were obtained as a pure lyophilized species and were reconstituted in PBS prior to use.

Biolayer Interferometry (Octet). Biotinylated peptides (100 nM) were loaded on streptavidin biosensors (Pall ForteBio) to a load threshold of 0.1 nm. Sensors were immediately regenerated in 100 mM glycine (pH 1.5) and neutralized to remove aggregates and nonspecific interactions. Ligand-loaded sensors were dipped into known concentrations of 5-Helix for an association step of 60 min. Then, 5-Helix was purified by size exclusion on the same day as the biolayer interferometry measurements. All reactions were run in PBS with 0.1% bovine serum albumin, 0.05% Tween 20, and 1 M guanidine hydrochloride. All samples in all experiments were baseline-subtracted to a well that loaded the tip with biotinylated ligand but did not go into sample, as a control for any buffer trends within the samples. The reported K_D values were computed using steady-state analysis in Octet software (Sartorius) are averaged across experiments repeated on two separate days.

Data, Materials, and Software Availability. All data in this manuscript is presented in either main text figures or *SI Appendix*.

ACKNOWLEDGMENTS. We thank members of the Kim Lab for critical reading of this manuscript. B.N.B. was supported by the NSF GRFP. T.U.J.B. was supported by the Knight-Hennessy Graduate Scholarship and a Canadian Institutes of Health Research Doctoral Foreign Study Award (FRN:170770). This work was supported by the Virginia and D. K. Ludwig Fund for Cancer Research, the Chan Zuckerberg Biohub, and an NIH Director's Pioneer Award (DP1AI158125) to P.S.K. Fig. 1 and *SI Appendix,* Fig. S1 were created using Biorender.

Author affiliations: [a]Department of Molecular and Cellular Physiology, Stanford University School of Medicine, Stanford, CA 94305; [b]Sarafan ChEM-H, Stanford University, Stanford, CA 94305; [c]Department of Biochemistry, Stanford University School of Medicine, Stanford, CA 94305; and [d]Chan Zuckerberg Biohub, San Francisco, CA 94158

1. M. S. Seaman *et al.*, Tiered categorization of a diverse panel of HIV-1 Env pseudoviruses for assessment of neutralizing antibodies. *J. Virol.* **84**, 1439–1452 (2010).
2. P. Hraber, B. Korber, K. Wagh, D. Montefiori, M. Roederer, A single, continuous metric to define tiered serum neutralization potency against HIV. *eLife* **7**, e31805 (2018).
3. D. R. Burton, L. Hangartner, Broadly neutralizing antibodies to HIV and their role in vaccine design. *Annu. Rev. Immunol.* **34**, e31805 (2016).
4. J. M. Kovacs *et al.*, HIV-1 envelope trimer elicits more potent neutralizing antibody responses than monomeric gp120. *Proc. Natl. Acad. Sci. U.S.A.* **109**, 12111–12116 (2012).
5. Y. Qin *et al.*, Eliciting neutralizing antibodies with gp120 outer domain constructs based on M-group consensus sequence. *Virology* **462–463**, 363–376 (2014).
6. K. O. Saunders *et al.*, Vaccine induction of heterologous tier 2 HIV-1 neutralizing antibodies in animal models. *Cell Rep.* **21**, 3681–3690 (2017).

7. E. T. Crooks *et al.*, Vaccine-elicited tier 2 HIV-1 neutralizing antibodies bind to quaternary epitopes involving glycan-deficient patches proximal to the CD4 binding site. *PLoS Pathog.* **11**, e1004932 (2015).
8. M. Pauthner *et al.*, Elicitation of robust tier 2 neutralizing antibody responses in nonhuman primates by HIV envelope trimer immunization using optimized approaches. *Immunity* **46**, 1073–1088.e6 (2017).
9. J. H. Lee, G. Ozorowski, A. B. Ward, Cryo-EM structure of a native, fully glycosylated, cleaved HIV-1 envelope trimer. *Science* **351**, 1043–1048 (2016).
10. M. M. Shaik *et al.*, Structural basis of coreceptor recognition by HIV-1 envelope spike. *Nature* **565**, 318–323 (2019).
11. D. C. Chan, D. Fass, J. M. Berger, P. S. Kim, Core structure of gp41 from the HIV envelope glycoprotein. *Cell* **89**, 263–273 (1997).
12. V. Buzon *et al.*, Crystal structure of HIV-1 gp41 including both fusion peptide and membrane proximal external regions. *PLoS Pathog.* **6**, e1000880 (2010).
13. D. M. Eckert, P. S. Kim, Mechanisms of viral membrane fusion and its inhibition. *Annu. Rev. Biochem.* **70**, 777–810 (2001).
14. S. C. Harrison, Viral membrane fusion. *Virology* **479–480**, 498–507 (2015).
15. J. M. White, S. E. Delos, M. Brecher, K. Schornberg, Structures and mechanisms of viral membrane fusion proteins: Multiple variations on a common theme. *Crit. Rev. Biochem. Mol. Biol.* **43**, 189–219 (2008).
16. F. A. Rey, S.-M. Lok, Common features of enveloped viruses and implications for immunogen design for next-generation vaccines. *Cell* **172**, 1319–1334 (2018).
17. Z. Yang, H. Wang, A. Z. Liu, H. B. Gristick, P. J. Bjorkman, Asymmetric opening of HIV-1 Env bound to CD4 and a coreceptor-mimicking antibody. *Nat. Struct. Mol. Biol.* **26**, 1167– 1175 (2019).
18. M. S. Ladinsky *et al.*, Electron tomography visualization of HIV-1 fusion with target cells using fusion inhibitors to trap the pre-hairpin intermediate. *eLife* **9**, e58411 (2020).
19. D. C. Montefiori *et al.*, The high-affinity immunoglobulin receptor FcγRI potentiates HIV-1 neutralization via antibodies against the gp41 N-heptad repeat. *Proc. Natl. Acad. Sci. U.S.A.* **118**, e2018027118 (2021).
20. A. A. Rubio *et al.*, A derivative of the D5 monoclonal antibody that targets the gp41 N-heptad repeat of HIV-1 with broad tier-2-neutralizing activity. *J. Virol.* **95**, e0235020 (2021).
21. M. J. Root, M. S. Kay, P. S. Kim, Protein design of an HIV-1 entry inhibitor. *Science* **291**, 884–888 (2001).
22. D. C. Chan, P. S. Kim, HIV entry and its inhibition. *Cell* **93**, 681–684 (1998).
23. M. Pancera *et al.*, Structure and immune recognition of trimeric pre-fusion HIV-1 Env. *Nature* **514**, 455–461 (2014).
24. M. Pancera, A. Changela, P. D. Kwong, How HIV-1 entry mechanism and broadly neutralizing antibodies guide structure-based vaccine design. *Curr. Opin. HIV AIDS* **12**, 229–240 (2017).
25. X. Wu *et al.*, Rational design of envelope identifies broadly neutralizing human monoclonal antibodies to HIV-1. *Science* **329**, 856–861 (2010).
26. K. Xu *et al.*, Epitope-based vaccine design yields fusion peptide-directed antibodies that neutralize diverse strains of HIV-1. *Nat. Med.* **24**, 857–867 (2018).
27. K. O. Saunders *et al.*, Vaccine Elicitation of high mannose-dependent neutralizing antibodies against the V3-glycan broadly neutralizing epitope in nonhuman primates. *Cell Rep.* **18**, 2175–2188 (2017).
28. M. Caskey *et al.*, Antibody 10–1074 suppresses viremia in HIV-1-infected individuals. *Nat. Med.* **23**, 185–191 (2017).
29. M. Caskey *et al.*, Viraemia suppressed in HIV-1-infected humans by broadly neutralizing antibody 3BNC117. *Nature* **522**, 487–491 (2015).
30. L. Corey *et al.*, Two randomized trials of neutralizing antibodies to prevent HIV-1 acquisition. *N. Engl. J. Med.* **384**, 1003–1014 (2021).
31. S. Mahomed, N. Garrett, C. Baxter, Q. Abdool Karim, S. S. Abdool Karim, Clinical trials of broadly neutralizing monoclonal antibodies for human immunodeficiency virus prevention: A review. *J. Infect. Dis.* **223**, 370–380 (2021).
32. C. T. Wild, D. C. Shugars, T. K. Greenwell, C. B. McDanal, T. J. Matthews, Peptides corresponding to a predictive alpha-helical domain of human immunodeficiency virus type 1 gp41 are potent inhibitors of virus infection. *Proc. Natl. Acad. Sci. U.S.A.* **91**, 9770–9774 (1994).
33. D. M. Eckert, P. S. Kim, Design of potent inhibitors of HIV-1 entry from the gp41 N-peptide region. *Proc. Natl. Acad. Sci. U.S.A.* **98**, 11187–11192 (2001).
34. D. M. Eckert, V. N. Malashkevich, L. H. Hong, P. A. Carr, P. S. Kim, Inhibiting HIV-1 entry: Discovery of D-peptide inhibitors that target the gp41 coiled-coil pocket. *Cell* **99**, 103–115 (1999).
35. B. D. Welch *et al.*, Design of a potent D-peptide HIV-1 entry inhibitor with a strong barrier to resistance. *J. Virol.* **84**, 11235–11244 (2010).
36. A. Lazzarin *et al.*, Efficacy of enfuvirtide in patients infected with drug-resistant HIV-1 in Europe and Australia. *N. Engl. J. Med.* **348**, 2186–2195 (2003).
37. J. P. Lalezari *et al.*, Enfuvirtide, an HIV-1 fusion inhibitor, for drug-resistant HIV infection in North and South America. *N. Engl. J. Med.* **348**, 2175–2185 (2003).
38. C. Sabin *et al.*, Crystal structure and size-dependent neutralization properties of HK20, a human monoclonal antibody binding to the highly conserved heptad repeat 1 of gp41. *PLoS Pathog.* **6**, e1001195 (2010).
39. B. Foley *et al.*, *HIV Sequence Compendium 2018* (Los Alamos National Laboratory, Theoretical Biology and Biophysics, Los Alamos, New Mexico, 2018).
40. A. deCamp *et al.*, Global panel of HIV-1 Env reference strains for standardized assessments of vaccine-elicited neutralizing antibodies. *J. Virol.* **88**, 2489–2507 (2014).
41. H. K. Steger, M. J. Root, Kinetic dependence to HIV-1 entry inhibition. *J. Biol. Chem.* **281**, 25813–25821 (2006).
42. K. M. Kahle, H. K. Steger, M. J. Root, Asymmetric deactivation of HIV-1 gp41 following fusion inhibitor binding. *PLoS Pathog.* **5**, e1000674 (2009).
43. M. D. Khasnis, K. Halkidis, A. Bhardwaj, M. J. Root, Receptor activation of HIV-1 Env leads to asymmetric exposure of the gp41 trimer. *PLoS Pathog.* **12**, e1006098 (2016).
44. K. W. Ahn, M. J. Root, Complex interplay of kinetic factors governs the synergistic properties of HIV-1 entry inhibitors. *J. Biol. Chem.* **292**, 16498–16510 (2017).
45. D. C. Montefiori, M. Roederer, L. Morris, M. S. Seaman, Neutralization tiers of HIV-1. *Curr. Opin. HIV AIDS* **13**, 128–136 (2018).
46. D. Sok *et al.*, Recombinant HIV envelope trimer selects for quaternary-dependent antibodies targeting the trimer apex. *Proc. Natl. Acad. Sci. U.S.A.* **111**, 17624–17629 (2014).
47. J. F. Scheid *et al.*, Sequence and structural convergence of broad and potent HIV antibodies that mimic CD4 binding. *Science* **333**, 1633–1637 (2011).
48. H. Mouquet *et al.*, Complex-type N-glycan recognition by potent broadly neutralizing HIV antibodies. *Proc. Natl. Acad. Sci. U.S.A.* **109**, E3268–E3277 (2012).
49. Y. D. Kwon *et al.*, Optimization of the solubility of HIV-1-neutralizing antibody 10E8 through somatic variation and structure-based design. *J. Virol.* **90**, 5899–5914 (2016).
50. D. C. Montefiori, "Measuring HIV neutralization in a luciferase reporter gene assay" in *HIV Protocols, Methods in Molecular Biology*, V. R. Prasad, G. V. Kalpana, Eds. (Humana Press, 2009), pp. 395–405.
51. D. A. Ozaki *et al.*, International technology transfer of a GCLP-compliant HIV-1 neutralizing antibody assay for human clinical trials. *PLoS One* **7**, e30963 (2012).
52. C. A. Todd *et al.*, Development and implementation of an international proficiency testing program for a neutralizing antibody assay for HIV-1 in TZM-bl cells. *J. Immunol. Methods* **375**, 57–67 (2012).
53. M. Sarzotti-Kelsoe *et al.*, Optimization and validation of the TZM-bl assay for standardized assessments of neutralizing antibodies against HIV-1. *J. Immunol. Methods* **409**, 131–146 (2014).
54. E. M. Fenyö *et al.*, International network for comparison of HIV neutralization assays: The NeutNet report. *PLoS One* **4**, e36438 (2009).
55. T. Moyo *et al.*, Molecular basis of unusually high neutralization resistance in tier 3 HIV-1 strain 253–11. *J. Virol.* **92**, e02261-17 (2018).
56. R. T. van Dorsten *et al.*, Neutralization breadth and potency of single-chain variable fragments derived from broadly neutralizing antibodies targeting multiple epitopes on the HIV-1 envelope. *J. Virol.* **94**, e01533-19 (2020).
57. J. D. Reeves *et al.*, Enfuvirtide resistance mutations: Impact on human immunodeficiency virus envelope function, entry inhibitor sensitivity, and virus neutralization. *J. Virol.* **79**, 4991–4999 (2005).
58. H. Yoon *et al.*, CATNAP: A tool to compile, analyze and tally neutralizing antibody panels. *Nucleic Acids Res.* **43**, W213–W219 (2015).
59. G. Frey *et al.*, A fusion-intermediate state of HIV-1 gp41 targeted by broadly neutralizing antibodies. *Proc. Natl. Acad. Sci. U.S.A.* **105**, 3739–3744 (2008).
60. H. M. Schapiro *et al.*, Regulation of epitope exposure in the gp41 membrane-proximal external region through interactions at the apex of HIV-1 Env. *PLOS Pathog.* **18**, e1010531 (2022).
61. D. R. Burton, A new lease on life for an HIV-neutralizing antibody class and vaccine target. *Proc. Natl. Acad. Sci. U.S.A.* **118**, e2026390118 (2021).
62. M. Pope, A. T. Haase, Transmission, acute HIV-1 infection and the quest for strategies to prevent infection. *Nat. Med.* **9**, 847–852 (2003).
63. D. J. Stieh *et al.*, Th17 cells are preferentially infected very early after vaginal transmission of SIV in macaques. *Cell Host Microbe* **19**, 529–540 (2016).
64. D. J. Stieh *et al.*, Vaginal challenge with an SIV-based dual reporter system reveals that infection can occur throughout the upper and lower female reproductive tract. *PLoS Pathog.* **10**, e1004440 (2014).
65. J. Hu, M. B. Gardner, C. J. Miller, Simian immunodeficiency virus rapidly penetrates the cervicovaginal mucosa after intravaginal inoculation and infects intraepithelial dendritic cells. *J. Virol.* **74**, 6087–6095 (2000).
66. R. Shen *et al.*, Macrophages in vaginal but not intestinal mucosa are monocyte-like and permissive to human immunodeficiency virus type 1 infection. *J. Virol.* **83**, 3258–3267 (2009).
67. A. Smed-Sörensen *et al.*, Differential susceptibility to human immunodeficiency virus type 1 infection of myeloid and plasmacytoid dendritic cells. *J. Virol.* **79**, 8861–8869 (2005).
68. J. B. Munro *et al.*, Conformational dynamics of single HIV-1 envelope trimers on the surface of native virions. *Science* **346**, 759–763 (2014).
69. X. Ma *et al.*, HIV-1 Env trimer opens through an asymmetric intermediate in which individual protomers adopt distinct conformations. *eLife* **7**, e34271 (2018).
70. J. D. Reeves *et al.*, Sensitivity of HIV-1 to entry inhibitors correlates with envelope/coreceptor affinity, receptor density, and fusion kinetics. *Proc. Natl. Acad. Sci. U.S.A.* **99**, 16249–16254 (2002).
71. D. M. Eckert *et al.*, Characterization of the steric defense of the HIV-1 gp41 N-trimer region. *Protein Sci.* **17**, 2091–2100 (2008).
72. A. E. Hamburger, S. Kim, B. D. Welch, M. S. Kay, Steric accessibility of the HIV-1 gp41 N-trimer region. *J. Biol. Chem.* **280**, 12567–12572 (2005).
73. P. B. Gilbert *et al.*, Neutralization titer biomarker for antibody-mediated prevention of HIV-1 acquisition. *Nat. Med.* **28**, 1924–1932 (2022).
74. R. Zhang *et al.*, Initiation of immune tolerance–controlled HIV gp41 neutralizing B cell lineages. *Sci. Transl. Med.* **8**, 336ra62 (2016).
75. L. G. Perez, M. R. Costa, C. A. Todd, B. F. Haynes, D. C. Montefiori, Utilization of immunoglobulin G Fc receptors by human immunodeficiency virus type 1: A specific role for antibodies against the membrane-proximal external region of gp41. *J. Virol.* **83**, 7397–7410 (2009).
76. L. G. Perez, S. Zolla-Pazner, D. C. Montefiori, Antibody-dependent, FcγRI-mediated neutralization of HIV-1 in TZM-bl cells occurs independently of phagocytosis. *J. Virol.* **87**, 5287–5290 (2013).
77. B. N. Bell, A. E. Powell, C. Rodriguez, J. R. Cochran, P. S. Kim, Neutralizing antibodies targeting the SARS-CoV-2 receptor binding domain isolated from a naïve human antibody library. *Protein Sci.* **30**, 716–727 (2021), 10.1002/pro.4044.